Available online at www.sciencedirect.com

ScienceDirect

Procedia Materials Science 3 (2014) 1298 – 1303

Procedia Materials Science

www.elsevier.com/locate/procedia

20th European Conference on Fracture (ECF20)

Numerical study of spall fracture in solids subjected to high strain rate loading

Siva Prasad AVS, Sumit Basu*

Department of Mechanical Engineering, Indian Institute of Technology Kanpur, Kanpur and 208106, India.

Abstract

Experimental and numerical investigations to understand the mechanisms of spall fracture of solids subjected to high strain rate loading have been going on for several decades. While microscopic studies of the fractured samples from experiments provide information on the final microstructure and distribution of the voids or cracks on the fractured surface, numerical simulations help construct and validate theories to explain the fracture phenomenon. In the present work, numerical simulations of plate impact are performed to study the role of fracture modes and thermal softening effects on the free surface velocity profiles. Two damage models based on critical mean stress and critical principal stress, representing ductile and brittle fracture respectively, are used for the target plate. The depth of pullback signals in the free surface velocity profiles are predicted for the above parameters.

Selection and peer-review under responsibility of the Norwegian University of Science and Technology (NTNU), Department of Structural Engineering

Keywords: Spall fracture; free surface velocity; Smoothed Particle Hydrodynamics (SPH)

1. Introduction

Characterization of materials subjected to high pressures and strain rates is very important in the light of increased demand for advanced materials which can withstand shock and blast loading encountered in military as well as civilian applications. The material response in such extreme situations significantly differs from quasi-static loading. Materials which undergo large plastic deformation in the low strain rate regime may display brittle fracture behaviour at high strain rates. Typical load rise times and fracture times involved in such loadings are in the order $\sim 1\ \mu$s. A detailed review of methodology and mechanisms of spall fracture of different materials and the experimental methods employed can be found in Kanel (2010) and Antoun et al. (2003). Flyer plate impact and expanding ring experiments are used to study the material response at very high strain rates. In a plate impact experiment, due to the uniaxial plane strain loading situation, mechanical properties like yield strength and fracture strength can be determined by measuring the velocity at the target free surface (v_{fs}). A typical free surface velocity profile may contain the signature of the occurrence of various phenomena in the bulk of the target material, like plastic shock deformation, phase transforma-

* Corresponding author. Tel.: +91-512-259-6034 ; fax: +91-512-259-7408.
E-mail address: sbasu@iitk.ac.in

Selection and peer-review under responsibility of the Norwegian University of Science and Technology (NTNU), Department of Structural Engineering
doi:10.1016/j.mspro.2014.06.210

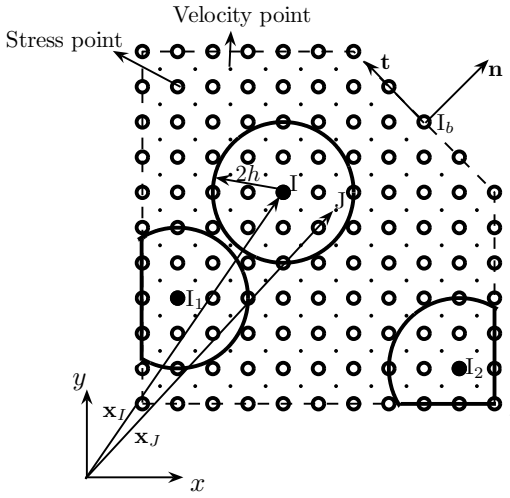

Fig. 1. Typical discretization of a domain using velocity points (·) and stress points (∘).

tion, thermal softening and fracture. Microscopic studies of the fractured surfaces of the samples from experiments help arriving at an explanation of possible mechanism of failure. However, numerical simulations are required to help comprehend the physics of deformation in the bulk of the material since the entire deformation history is available everywhere in the domain. Thus, deciphering the v_{fs} profile requires a systematic analytical or numerical study of the plate impact problem.

Given that large deformation and fragmentation are observed in dynamic loading situations, a meshless method is a more convenient numerical tool than grid based methods to simulate such phenomena. Smoothed Particle Hydrodynamics (SPH) is a Lagrangian particle method in which the gradients of the field variables are approximated with the help of a smoothing function (Liu and Liu , 2003). SPH has the capability to deal with material separation and fragmentation in a more realistic manner due its particle nature. The objective of the present work is to perform numerical simulations to study the effect of ductile and brittle fracture modes and thermal softening on v_{fs} profile, particularly, the pullback signal and the residual velocity of the fractured material. A two dimensional (2-D) code based on the meshless method Smoothed Particle Hydrodynamics (SPH) is developed and used for the numerical simulations. Copper is chosen as a representative material for our simulations. In section 2, the SPH equations, the constitutive model and the damage laws are briefly explained. The results of the numerical simulations are discussed, relating the mechanics of wave interactions in the bulk of the target material to the free surface velocity profile, in section 3.

2. Computational methodology and constitutive equations

2.1. SPH formulation

In this work, the problem domain is discretized into stress points and velocity points (Fig. 1) as proposed by Randles and Libersky (2000). The SPH approximations for balance of mass, linear momentum and energy, assuming zero body forces and adiabatic deformation, are given as (Randles and Libersky , 1996)

$$\frac{D\rho_{\mathrm{I}}}{Dt} = -\rho_{\mathrm{I}}\mathbf{l}_{\mathrm{I}} : \mathbf{I}, \tag{1a}$$

$$\frac{D\boldsymbol{v}_{\mathrm{I}}}{Dt} = \left(\sum_{\mathrm{J}} \frac{m_{\mathrm{J}}}{\rho_{\mathrm{I}}\rho_{\mathrm{J}}} \left(\boldsymbol{\Sigma}_{\mathrm{J}} - \boldsymbol{\Sigma}_{\mathrm{I}}\right) \otimes \boldsymbol{\nabla} W_{\mathrm{IJ}}\right) : \boldsymbol{B}_{\mathrm{I}}^{-1}, \text{ and} \tag{1b}$$

$$\frac{De_{\mathrm{I}}}{Dt} = \frac{1}{\rho_{\mathrm{I}}}\boldsymbol{\Sigma}_{\mathrm{I}} : \mathbf{l}_{\mathrm{I}}, \tag{1c}$$

where, m_{I}, ρ_{I}, $\boldsymbol{\Sigma}_{\mathrm{I}}$, v_{I}, $\mathbf{l}_{\mathrm{I}}$ and e are the mass, density, macroscopic Cauchy stress tensor, velocity, velocity gradient tensor and specific internal energy on each point. W_{IJ} is a smoothing function for which a cubic B-spline function (eq. (2)) is chosen in this work.

$$W(s) = \frac{10}{7\pi h^2} \begin{cases} 1 - \frac{3}{2}s^2 + \frac{3}{4}s^3, & 0 \le s \le 1 \\ \frac{1}{4}(2-s)^3, & 1 \le s \le 2 \\ 0, & s > 2, \end{cases} \tag{2}$$

where, $s = r_{\mathrm{IJ}}/h$, $r_{\mathrm{IJ}} = |\mathbf{x}_{\mathrm{I}} - \mathbf{x}_{\mathrm{J}}|$ and h is the mean of the smoothing lengths of points I and J. $\boldsymbol{B}_{\mathrm{I}}$ is a correction to account for incomplete support domains of points close to or on the boundary of the domain (I_1, I_2 in Fig. 1), given by $\boldsymbol{B}_{\mathrm{I}} = \sum_{\mathrm{J}} \frac{m_{\mathrm{J}}}{\rho_{\mathrm{J}}} (\mathbf{x}_{\mathrm{J}} - \mathbf{x}_{\mathrm{I}}) \otimes \boldsymbol{\nabla} W_{\mathrm{IJ}}$ and the velocity gradient tensor, $\mathbf{l}_{\mathrm{I}}$ on a point I, required in eq. (1a) and eq. (1c), is given by $\mathbf{l}_{\mathrm{I}} = \left(\sum_{\mathrm{J}} \frac{m_{\mathrm{J}}}{\rho_{\mathrm{J}}} (\boldsymbol{v}_{\mathrm{J}} - \boldsymbol{v}_{\mathrm{I}}) \otimes \boldsymbol{\nabla} W_{\mathrm{IJ}}\right) \cdot \boldsymbol{B}_{\mathrm{I}}^{-1}$. Stress points carry velocity gradient tensor, stresses, densities, specific internal energies, damage and equivalent plastic strain. Velocity points carry velocities and accelerations. Standard Verlet-Leapfrog algorithm is used for the time integration of eqs. (1a) - (1c). Damage is implemented in the numerical model by disregarding a completely damaged stress point in the SPH calculations (eqs. (1a) - (1c)).

2.2. Constitutive equations

The material is chosen to be elastic-viscoplastic, with the hydrostatic part being calculated using Mie-Grüneisen equation of state. In terms of the Jaumann rate of Kirchoff stress tensor ($\boldsymbol{\tau} = \frac{\rho_0}{\rho}\boldsymbol{\Sigma}$), the complete constitutive equation is

$$\overset{\nabla}{\boldsymbol{\tau}} = K(\mathbf{d} : \mathbf{I})\mathbf{I} + 2\mu\mathbf{d}' - \frac{3\mu}{\Sigma_e}\dot{\epsilon}^p\boldsymbol{\tau}', \tag{3}$$

where, $\mathbf{d}_{\mathrm{I}}$ is the strain rate tensor, $\mathrm{K} = -\left(1 + \frac{1}{2}\Gamma_0\right)\frac{p_H(\chi)}{1+\chi} + \left(1 - \frac{1}{2}\Gamma_0\chi\right)\frac{dp_H}{d\chi}$, $\chi = \rho/\rho_0 - 1$, ρ_0 is the initial density, μ is the shear modulus, p_H is the reference pressure on the $p - \rho$ Hugoniot of the material, Σ_e is the macroscopic equivalent stress. $\dot{\epsilon}^p$ is the equivalent plastic strain rate given by, $\dot{\epsilon}^p = \dot{\epsilon}_0^p \left(\frac{\Sigma_e}{g(\epsilon^p, T)}\right)^{1/m}$, where, $g(\epsilon^p, T) = \Sigma_0 \left(1 + \frac{\epsilon^p}{\epsilon_0^p}\right)^N \left(1 - \left(\frac{T - T_0}{T_m - T_0}\right)^{m_j}\right)$. Here, ϵ^p is the equivalent plastic strain, Σ_0 is the initial yield stress, ϵ_0^p is the strain at initial yield and $\dot{\epsilon}_0^p$ is the reference plastic strain rate. T_0 and T_m are the reference and melting point temperatures respectively. N, m and m_j are hardening, strain rate sensitivity and thermal softening exponents respectively.

In the present study, the damage models based on the critical mean stress and the critical principal stress are used to investigate the ductile and the brittle fracture modes, respectively. For the damage model based on critical mean stress, the void growth relation derived by Johnson (1981) with inertia term included is used. A damage variable D, is defined as $\mathrm{D} = \left(\frac{f}{f_{\mathrm{cr}}}\right)^n$, where f is the void volume fraction, f_{cr} is the critical void volume fraction and n is the exponent which controls the rate of damage growth. The evolution of f is given by the equation

$$\Delta p = \rho_m \left(\frac{1 - f_0}{f_0} a_0^3\right)^{2/3} \left\{ \frac{1 - f^{1/3}}{3f^{1/3}(1-f)^{5/3}} \ddot{f} - \frac{2}{9} \frac{\dot{f}^2}{f^{4/3}(1-f)^{8/3}} \left(\frac{1}{4}\left(1 - f^{4/3}\right) - 3f + f^{1/3}\right)\right\}, \tag{4}$$

where, f_0 and a_0 are the initial void volume fraction and void radius, taken uniform throughout the domain and $\Delta p = \frac{\Sigma_{kk}}{3(1-f)} - \frac{2}{3}\sigma_0 \ln\left(\frac{1}{f}\right) - \eta\left(\frac{1-f_0}{f_0}\right)^{2/3} \frac{\dot{f}}{f^{1/3}(1-f)^{5/3}}$. $\dot{f} = 0$ when $\Delta p \le 0$. σ_0, ρ_m and η are the initial yield stress, density and viscosity coefficient of the matrix material respectively. The first term on the right hand side of the above

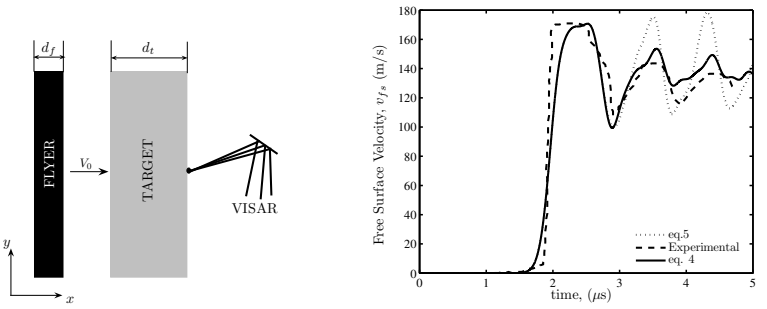

(a) (b)

Fig. 2. (a) Schematic of flyer plate impact setup, (b)Validation with experimental v_{fs} profiles.

equation represents the microscopic inertia, which has been included in order to see its effect at very high imapct velocities and strain rates. It has been found through our simulations that neglecting this term at high strain rates results in a shallower pullback signal on the free surface velocity profle and thus, the spall strength of the material is underestimated. The second order ordinary differential equation (ODE) in f, eq. (4), is solved using the fourth order Runge-Kutta (RK) method. To simulate brittle fracture mode, a phenomenological damage law based on critical principal stress (Randles and Libersky , 1996) is used in this work.

$$\dot{\mathrm{D}} = \begin{cases} \left[\left(\Sigma_1 - \Sigma^{\mathrm{th}}\right)/\Sigma_0^{\mathrm{th}}\right]^2 / \left[t_d\left(1-\mathrm{D}^2\right)\right], & \Sigma_1 > \Sigma^{\mathrm{th}} \\ 0, & \Sigma_1 \leq \Sigma^{\mathrm{th}}, \end{cases} \tag{5}$$

where, Σ_1 is the maximum of the three principal stresses, Σ_0^{th} and $\Sigma^{th}\left(=(1-\mathrm{D})\,\Sigma_0^{th}\right)$ are the initial and the current threshold stresses of the material, respectively.

3. Numerical simulations and results

A 2-D SPH code has been developed based on the formulation and the constitutive model discussed in sections 2.1 and 2.2. A schematic of flyer plate impact experiment is shown in Fig. 2(a). The impact is called symmetric when the target and the flyer are of same material. The code thus developed is validated (Fig. 2(b)) with the experimental v_{fs} profile provided in Rajendran et al. (1989) for a Copper on Copper plate impact at a velocity $V_0 = 185$ m/s. With reference to Fig. 2(a), the thicknesses of the target and the flyer plates are respectively, $d_t = 9$ mm and $d_f = 2$ mm. It can be noticed that the time of spall signature recorded in experiment matches with that in simulations with both the damage models (eq. (4) and eq. (5)).

Having validated the numerical model, simulations of Copper on Copper symmetric plate impact is performed at an impact velocity $V_0 = 600$ m/s to relate the shock response in the bulk of the target material to the signature on the free surface velocity profile. Fig. 3(a) shows the v_{fs} profiles for the cases when no spall is included in the numerical model (grey line), ductile fracture mode is modelled without thermal softening (solid line) and with thermal softening (dashed line) and brittle fracture is modelled (dotted line). Upon impact, compressive shock waves propagate into the target and flyer plates. Interaction of the shock wave with the free surface of the flyer plate results in a rarefaction wave propagating back, reducing the shock stress to 0. The rarefaction wave continues propagating into the target without undergoing any change since both the plates are of the same material. The shock wave in the flyer also interacts with the target free surface, resulting in a rarefaction wave. A tensile state of stress is created at a point in the bulk of the target plate upon the interaction of these rarefaction waves. This location is the potential site for fracture and is called spall plane. If no fracture is included in the model, this tensile stress expands as a square pulse on either sides of the spall plane, throughout the thickness of the target. Upon the interaction of the tensile pulse with the target free surface, the velocity of the free surface starts decreasing and reaches to a minimum (grey line in Fig. 3(a)), depending upon the magnitude of the tensile pulse.

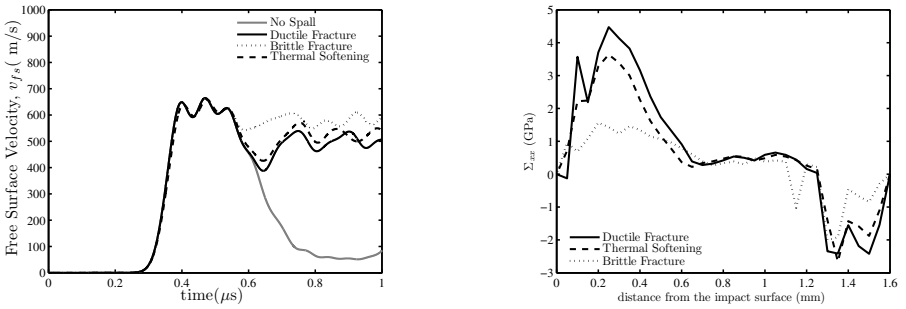

(a) (b)

Fig. 3. (a) v_{fs} profiles for V_0 = 600 m/s and (b) Σ_{xx} variation along the thickness of target.

When ductile fracture is modelled using eq. (4), critical mean stress based model (solid line in Fig. 3(a)), damage initiates as soon as the tensile mean stress exceeds the threshold mean stress and continues to evolve. As a result of damage softening, two triangular pulses start propagating from the spall plane towards the impact and the free surface of the target. The rear part of each triangular pulse is the signal of damage initiation. The triangular pulse that reaches the target free surface results in a compressive triangular pulse that starts propagating back into the target plate (Fig. 3(b)). Thus, the free surface velocity first starts decreasing upon the arrival of the tensile pulse and then, starts increasing as the compressive pulse recedes, registering the spall signature. This fall and rise of v_{fs} is called pullback signal. The rise in v_{fs} depends on the magnitude of the compressive pulse and the time taken for the damage completion signal to reach the free surface. When the damage completion signal reaches the target free surface, v_{fs} stops rising and the separated material flies at this residual velocity.

Effect of brittle fracture mode on the v_{fs} profile is studied by using eq. (5) as the fracture criterion. In plane wave propagation, where the deformation is uniaxial, the maximum tensile principal stress is greater than the mean tensile stress. As a result, damage initiation occurs much earlier than in ductile fracture mode. Hence a shallower pullback signal is registered in the v_{fs} profile (dotted line in Fig. 3(a)). The v_{fs} almost rises to the initial free surface velocity corresponding to shock, indicating brittle fracture at the spall plane. Thus, the residual velocity of the fractured material is higher in brittle fracture mode.

When thermal softening is also included in the ductile fracture model, the damage initiation is found to precede, showing a shallower pullback signal compared to when no thermal softening is included. However, the spall signal is still deeper than that for a brittle fracture case. The residual velocity in this case is a little higher compared to no softening case.

Due to plastic deformation, the magnitude of compressive pulse generated is not equal to that of the tensile pulse in the ductile fracture mode. As a result, the residual velocity is lower than in brittle fracture mode. In the case where thermal softening is included, the softening due to damage and temperature rise causes rapid damage growth. As a result the residual velocity is a little higher than with no softening, though the magnitude of compressive pulse is the same in both the cases. In brittle fracture mode, the damage growth rate is much higher than in the other two cases which results in much earlier spall initiation and completion, registering a shallower pullback signal and an almost complete rise in v_{fs}.

4. Summary and conclusions

Numerical simulations of symmetric plate impact is performed to understand and relate the shock wave Physics in the target material to the free surface velocity profile. The effect of brittle and ductile fracture modes and thermal softening are studied. Of all the three cases, brittle fracture mode recorded the shallowest pullback signal and the highest residual velocity in v_{fs} profile. In ductile fracture mode with no thermal softening, the pullback signal is deeper than with thermal softening. The residual velocity with thermal softening is higher than without thermal softening.

References

Antoun, T., Seaman, L., Curran, D., Kanel, G., Razorenov, S., Utkin, A., 2003. Spall Fracture. Springer, New York, Berlin, Heidelberg.

Johnson, J.N., 1981. Dynamic fracture and spallation in ductile solids. Journal of Applied Physics 52, 28122825.

Kanel, G., 2010. Spall fracture: methodological aspects, mechanisms and governing factors. International Journal of Fracture 163, 173191.

Liu, G., Liu, M., 2003. Smoothed Particle Hydrodynamics: a meshfree particle method. World Scientific, Singapore.

Randles, P., Libersky, L., 1996. Smoothed Particle Hydrodynamics: Some recent improvements and applications. Computer Methods in Applied Mechanics and Engineering 139, 375 408.

Rajendran, A.M., Dietenberger, M.A., Grove, D.J., 1989. A void growth-based failure model to describe spallation. Journal of Applied Physics 65, 15211527.

Randles, P.W., Libersky, L.D., 2000. Normalized SPH with stress points. International Journal for Numerical Methods in Engineering 48, 1445 1462.